Assessment of Climate Change Impact on Probable Maximum Floods in a Tropical Catchment

Saad Shauket Sammen (Saad123engineer@yahoo.com)
University of Diyala https://orcid.org/0000-0002-1708-0612
Thamer A Mohammed
University of Baghdad
Abdul Halim Ghazali
Universiti Putra Malaysia
Lariyah M Sidek
Universiti Teaaga Nasional, UNITEN
Shamsuddin Shahid
Universiti Teknologi Malaysia (UTM)
Sani Isah Abba
Baze University
Anurag Malik
Punjab Agricultural University, Regional Research Station

Research Article

Keywords: Probable maximum precipitation, probable maximum flood, hydrological model, climate change, hydrological extremes

Posted Date: August 13th, 2021

DOI: https://doi.org/10.21203/rs.3.rs-398782/v1

Version of Record: A version of this preprint was published at Theoretical and Applied Climatology on January 14th, 2022. See the published version at https://doi.org/10.1007/s00704-022-03925-9.

Abstract

Increased extreme rainfall due to climate change will increase the probable maximum flood (PMF) and pose a severe threat the critical hydraulic infrastructure like hydroelectric and flood protection dams. As the rainfall extremes in tropical regions are highly sensitive to global warming, increase PMF can be much higher in the tropics. A study has been conducted to assess the impact of climate change on PMF in a tropical catchment located in peninsular Malaysia. A lumped hydrological model, Mike NAM, is calibrated and validated with observed climate and inflow data of Tenmengor reservoir, located in the state of Perak of Peninsular Malaysia. Regional climate model projected rainfall is used to generate probable maximum precipitation (PMP) for future periods. The hydrological model is used to simulate PMF from PMP estimated for the historical and two future periods, early (2031–2045) and late (2060–2075). The results revealed the NAM model could simulate the river flow with a Nash–Sutcliffe efficiency of 0.74 and root mean square error of 0.51. The application of the model with projected rainfall revealed an increase in PMP by 162 to 507% and 259 to 487% during early and late periods for different return periods ranging from 5 to 1000 years. This would cause an increase in PMF by 48.9% and 122.6% during early and late periods. A large increase in PMF indicates the possibility of devastating floods in the study area due to climate change.

1. Introduction

Globally, floods share about 40% of total damage due to natural disasters (Noji, 1991). The frequency and severity of floods are more in a tropical region, and therefore, most of the damages due to floods are observed in tropical countries (Ohl & Tapsell, 2000). The majority of the tropical region receives a high amount of rainfall, which also varies with large-scale ocean-atmospheric cycles like other regions. However, the spatiotemporal rainfall variability in tropical regions is more affected by southern oscillation and Atlantic multi-decadal oscillation, which causes high rainfall in some seasons (Goly & Teegavarapu, 2013(. In El-Nina years, the high amounts of rainfall often occur as several extreme rainfall episodes that cause divesting floods.

Foods in most parts of the world have been projected to increase due to the increase in rainfall extremes driven by global warming-induced climate change (Change, 2014; Vitousek et al., 2017(. Rainfall extremes in tropical regions are highly sensitive to global warming. It has been estimated that a 1°C rise in temperature in tropical regions would cause 10% heavier rainfall extremes. Therefore, the probability of flooding is higher in these regions than in other parts of the world (Vitousek et al., 2017(. Increase rainfall extremes will increase the severity of floods, which may severely affect the economy and livelihood in the tropical region.

The flood occurs due to probable maximum precipitation (PMP) under a favorable catchment hydraulic condition (e.g., maximum moisture) is known as probable maximum floods (PMF). The PMP and PMF are essential for designing hydraulic structures for the mitigation of floods. It can be anticipated that increased rainfall extremes in tropical regions due to climate change will increase PMP and PMF (Beven,

2012; Rientjes, Muthuwatta, Bos, Booij, & Bhatti, 2013). Such information is vital for designing or retrofitting hydraulic structures for adaptation and mitigation to climate change. A general procedure of estimating PMF is the estimation of PMP by fitting distribution to extreme rainfall for different return periods, which is then used in a rainfall-runoff simulation model to generate PMF (Beven, 2012).

Rainfall-Runoff (R-R) models link rainfall (precipitation) with the watershed's runoff. Identifying the runoff from the rainfall events is required for investigating the forecasting of the streamflow from rainfall (Smith, 1965). Such forecasts are essential for deciding design factors of hydraulic infrastructures, early warnings of floods or droughts, operating reservoir or hydropower plants, and planning irrigation and water resources management activities (Bakhtiari, 2018; Ferraro, Costabile, Costanzo, Petaccia, & Macchione, 2020; Li et al., 2020; Ren, Hong, Li, Kang, & Li, 2020; Yang, Magnusson, Huang, Beldring, & Xu, 2020). The relationship between rainfall and runoff is always very difficult to be structured because of the immense spatial and temporal variability of rainfall and the physical characteristics of the watershed, as well as a few hydrological features of the watershed that should be included in the model process (Choi, Shin, & Kim, 2020; Gan, He, & Qin, 2020; Ling et al., 2019). Therefore, many R-R models have been developed over time based on a different concept (Kimura et al., 2019). The existing R-R models could be categorized into three main classes, empirical, conceptual and physical. These models can be classified into three major categories, physical, conceptual and empirical. Physically-based R-R models represent the 'physics' behind the catchment hydrological processes that generate runoff. Generally, these models employed the Partial Differential Equations (PDE) to propose an appropriate understanding of the catchment's R-R interrelationship and process (Ciupak, Ozga-Zielinski, Adamowski, Deo, & Kochanek, 2019; Song, Her, Suh, Kang, & Kim, 2019; Velázquez-Zapata, 2019). It should be noted that the used parameters and variables should be closely related to or identical with actual characteristics of catchment hydrological system for the physical-based model. Thus, physically-based models can represent the hydrologic state of a catchment at any time. Usually, these models are developed based on two or three-dimensional concepts, and hence, the required data to adequately develop the model is considerably huge compared with other model types. On the other hand, for the empirical models, the required data is the meteorological, physiography and the geology features at several locations along with the watershed (Farzin et al., 2018). On the other hands, for the identification of boundary condition mathematically, additional information about the nature and type of the catchment boundary conditions are necessary to be available (Rientjes et al., 2013).

In a conceptual model, relatively simple mathematical relations are used to understand a system's physics (Artificial Neural Networks in Hydrology. I: Preliminary Concepts, 2000). The main idea of conceptual models is that discharge has a relationship with storage through some transformation equations and conservation of mass equations (Rientjes et al., 2013). There are a few conceptual models procedures to consider the representations for the parameters and the variables to mimic the temporal and spatial distribution within the catchment. In this context, these model types used a simplified procedure as the one used in the physical-based model concept, while the others used the lumped concept, which is used in the empirical modeling concept. The conceptual modeling procedure can also

be referred to as grey-box models since they are considered as a hybridization of the empirical (black box) and physically-based (white box) models.

R-R models can be implemented completely within an analytical framework based on input and output observations of catchment water flow. The study area catchment could be considered as Black-Box packaging of features. Hence, there is no need to pay attention to the inner hydrological or meteorological process to detect the interrelationship between the rainfall and the runoff (Beven, 2012). These models are also called empirical models and are often recommended when the relationship between rainfall and runoff becomes difficult to describe with limited available data. Therefore, empirical models are often used for the catchment, where hydrological data and information are very limited. However, empirical models have several drawbacks which restrict their suitability. In the Black-Box model, the parameters (e.g. regression Coefficient) could be derived from the historical data. Thus, the model could only be used for the particular catchment. Besides, the validation of the model will remain only for the used time-period used for developing the model. As a result, the physically-based models are most widely used to predict probable maximum runoff due to PMP under climate change conditions.

The objective of the present study is to assess the impacts of climate change on PMF in a tropical catchment located in peninsular Malaysia. A physically-based hydrological model known as Mike NAM was used to simulate extreme runoff due to extreme rainfall. The PMP for historical (2001–2015) and two future periods (2031–2045 and 2060–2075) was estimated through probability distribution fitting of observed and regional climate model projected rainfall, respectively. The impact of climate change on hydrological extremes at regional and local scales is needed to assess since these vicissitudes are not uniform over the globe. It is expected that the information about possible impacts of climate change on PMF generated in this study would help in decision making in the planning and development of flood mitigation hydraulic structures.

2. Study Area And Data Collection

2.1. Study Area

Perak River is the second largest river in Peninsular Malaysia. It has an approximate length of 427 km and a catchment area of 15,180 km2, covering about 71% of the Perak state. The river's origin is in the mountains in the Northern part of Perak at an elevation of more than 2,000 m above the mean sea level. It flows southward from the origin and finally discharges to the Straits of Malacca in Bagan Datoh. Along the upper Perak river basin, there is a series of 4 hydropower dams at Temenggor, Bersia, Kenering and Chenderoh, known as the Perak River hydroelectric scheme. A catchment area of 3506 km2 feeds the Temengor reservoir. The elevation at the catchment area ranges from 206 m to 2156 m. The catchment is mostly forested and consists of a lake with a surface area of about 150 km2 known as Temengor lake. Figure 1 shows the location of the Temengor catchment on the map of peninsular Malaysia.

2.2. Data Acquisition

Rainfall and evaporation data are essential for modelling any hydrological processes. Daily rainfall data from eight rain gauges located within the Temengor catchment and evapotranspiration data from a meteorological station located in a nearby point were used for the development of a hydrological model in this study. There are no evapotranspiration measuring stations within the Temengor reservoir catchment area. Therefore, the evapotranspiration measuring station nearest to the study area (STN. PETAK UJIAN) is used in this study. Figure 2 shows the locations of rainfall gauges in the catchment. The details of each station are given in Table 1. The time series of rainfall data at different locations of the catchment are presented in Figure 2. Rainfall data are collected from the Department of Irrigation and Drainage (DID), Malaysia and the evapotranspiration data is collected Malaysian Meteorological Department. Temengor reservoir daily inflow data for the period 2007-2014 is used to calibrate and validate the model. Inflow data was collected from the Tenaga Nasional Berhad (TNB), Malaysia. Many streamflow and water level gauging stations are distributed along the Perak River, but most of the data collected from these stations were incomplete. Therefore, reservoir inflow data is used for calibration and validation of the hydrological model. The geospatial data, such as the digital elevation model (DEM) for the study area, was acquired from the National Energy Agency, Malaysia, which is used to identify the catchment boundary. Rainfall projections in the study area were acquired for 2010-2099 by the Regional Hydro-Climate Model of Peninsular Malaysia (RegHCM-PM) from the National Hydraulic Research Institute Malaysia (NAHRIM), Malaysia. The RegHCM-PM is the dynamically downscaled projections of the Canadian climate centre general circulation model CGCM1. The projected rainfall was used to assess the impact of climate change on inflow and PMP,

3. Methodology

The main objective of the hydrological model developed in this study is to simulate the Probable Maximum Flood (PMF). The PMF is important for designing hydraulic structures such as dams, channels and culverts. Figure 3 describes the methodology used in this study for the development of a hydrological model. A lumped conceptual model known as Mike Nedbor Afstromnings Model (NAM), developed by the Technical University of Denmark, was used for the hydrological modeling of the Temengor catchment. Hydrological model parameters cannot always be directly measured, and therefore, the conceptual models are often lumped on a catchment scale, and the catchment is considered as a single unit (Bakhtiari, 2018; Li et al., 2020; Smith, 1965). A lumped conceptual model was used in this study because it is simple but has a physical basis. The NAM model consists of four interrelated depots to mimic catchment storages: snow, surface, soil, and groundwater storage. The snow component was not considered as it does not occur in the catchment.

The daily rainfall, evapotranspiration and inflow data were collected for the period 2007-2014. Data for the period 2007-2011 was used for model calibration, and the data for the rest of three years (2012-2014) for model testing. Areal rainfall over the catchment was estimated using the Thiessen polygon method from the rain gauge estimations at 8 locations (Figure 4). For this purpose, the mean area weights or the proportion of rainfall that a station contributes to the catchment were determined and presented in Table 2. The Rainfall Intensity Duration Frequency (IDF) for different rainfall return periods was developed

using rainfall data for the period 2001-2015. The IDF was used to estimate PMP. Projected rainfall for future periods was also used for the projection of PMP for two future horizons, early (2031-2045) and late (2060-2075). The PMP of historical and future periods was used in the hydrological model for the generation of PMF to assess PMF changes in the Tenmongor catchment due to climate change.

3.1 Model Development

The Mike NAM model has the following basic input requirements.

- Catchment information (area of the catchments and the basic catchment composition)
- Meteorological data (rainfall and potential evapotranspiration)
- Hydrological data (discharge at the catchment outlets) for model validation and calibration
- Model parameters (threshold values and time constants for root zone storage, routing surface storage, and groundwater storage).

Unique values for rainfall, evapotranspiration and other parameters are considered for the development of the NAM model. The average values of the variables and parameters for the entire catchment are used for this purpose. Generally, it is difficult to estimate the parameter values based on the catchment's physiographic, climatic, and soil characteristics because most parameters are empirical and conceptual. Those values were determined by calibrating the hydrological model using hydrological time series.

The NAM model was calibrated with time-series data of catchment runoff to rainfall to determine the optimal model parameters. For modelling runoff of a day, rainfall and evapotranspiration for the present and the previous days, and the runoff of the previous day were used as model inputs.

3.2. Model Calibration and Validation

In this study, data for five years (2007- 2011) is used for model calibration. A combination of the automated and manual calibration was conducted for model calibration. The auto-calibration of the model is accomplished by optimizing four objective functions:

The negligible error between the average observed and simulated catchment runoff

A good agreement in the shape of the observed and simulated hydrograph (small root mean square error (RMSE)).

Good agreement between observed and simulated peak flow in terms of timing, rate, and volume.

A good relationship between the observed and simulated low flows

After the auto-calibration, nine model parameters were evaluated to show accurate agreement between the observed and simulated inflow. The calibrated model is then validated with observed data for the period (2012 – 2014).

3.3 Model Assessment

Both numerical and graphical approaches were utilized to assess the accuracy of the model. The graphical approach was used for interpretation, visualization, and qualitative evaluation of model outputs, while numerical evaluation was conducted objectively to assess the model performance. Besides, the statistical indices were used to assess the error and association between observed and modelled runoff. Many researchers gathered a list of performance indicators that are most commonly used in hydrologic modeling (Ehteram et al., 2018; Torabi Haghighi et al., 2019; Pham et al. 2021; Sammen et al. 2020; Mohamadi, S. et al. 2020; Tikhamarine et al. 2020). Some of those indicators including Mean Absolute Error (MAE), Percentage Bias (%BIAS), Root Mean Square Error (RMSE), Regression Coefficient (R2), Pearson Correlation Coefficient (PCC), Nash-Sutcliffe Coefficient of Efficiency (NSE), Flow Duration Error Index (EI), Index of Agreement defined by (IA) and the ratio of RMSE (RSE) are used in this study. The equation used to estimate the statistical indices, their range of values and the optimum value is given in Table 3.

3.4 Development of Rainfall Intensity Duration Frequency (IDF) Curves

IDF is a relationship between duration, intensity, and the rainfall's return period, which is often needed to plan and design different water resource projects. Several equations have been developed for the estimation of IDF. Frequency analysis techniques are often utilized to estimate the rainfall intensity for various return periods by using rainfall data.

In this study, the rainfall frequency's distribution is fitted with type I extreme value (Gumbel) distributions. The probability distribution function (PDF) is utilized to compute the observed rainfall intensity and duration for various return periods to generate the observed IDF curves. The PDF is then used to estimate maximum rainfall intensity for different durations for the return periods of 5, 10, 20, 50, 100, 500 and 1000 years.

3.5 Estimation of Probable Maximum Precipitation (PMP)

PMP in this study is developed using Harshfield Method. The Probable Maximum Precipitation (PMP) is defined as the highest depth of rainfall for a given duration that is meteorologically possible over a given station or a specified area [11]. The PMP for Malaysia is estimated using the Hershfield equation with a Km value equal to 15. But this value produced high rainfall depth, and therefore, is often considered very high for the country. A PMP study is conducted by NAHRIM (REF) for the whole of Malaysia to establish a standard method of PMP estimation through both statistical and hydrometeorological approaches. The average rainfall data of different stations for more than 20 years is used for this purpose. The study estimated the average value of Km for Perak state equal to 11.1. This value is used in this study to extract the PMP of the Tenmengor catchment.

4. Results And Discussion

4.1. Mike NAM Model Calibration

To model the runoff of the Temengor reservoir catchment, the NAM model is first calibrated using observed daily data for the period 2007-2011. Nine parameters of the NAM model are calibrated for accurate modelling of runoff. The list of the optimized parameters and their range is given in Table 4. The parameters values were optimized using input (rainfall and evapotranspiration) and the catchment's output (observed inflow) data. The optimum values for each parameter were then selected for the proposed model when the gap between the simulated and observed hydrograph was reduced.

The simulated and observed inflows for the Temenggor catchment are shown in Figure 5. It can be observed that the simulated model performed well during the calibration period. Figure 6 shows the simulated and observed peak flow for two high rainfall events. The figure reveals that the proposed model capable of simulating the peak inflow accurately during extreme rainfall events. However, the proposed model could not accurately simulate the inflow during the low flow period as the peak flow, as shown in Figure 7. One of the challenges of hydrological model calibration is that it is very difficult to accurately represent high and low inflow. Despite that, the emphasis in this study is given for accurate simulation of high inflow as flood forecasting is the study's main objective. The results revealed that the model could reflect the hydrological response of the Temenggor catchment to high rainfall for generating extreme flow.

Scatter plots(normal and log scales), as can be seen in Figure 8, are used to demonstrate the accuracy of the calibrated model in predicting the inflow hydrograph for the Temenggor catchment. The scatter plot in normal scale (Figure 8a) shows that all the points are concentrated along the diagonal line of the plot, which indicates the ability of the model to simulate all the values of observed inflow. The scatter plot in log-scale is prepared to present how the model can replicate the high and low flow. Figure 8b shows that all the high values are very close to the diagonal line of the plot, which indicates the ability of the model for accurate simulation of observed high flows. The low flow values were scattered, which means less capacity of the model to simulate the low flow accurately.

Figure 9 shows the observed and simulated inflow [(Qo – Qs)/Qo] against the observed inflow. The zero values in the plot reveal a good match between the simulated and the observed inflow. The figure shows zero relative residuals for high flow and very close to zero for medium flow. The relative residuals for the low flow values are high. This proves the superiority of the proposed model to simulate the high flow accurately.

To better present model capability, the monthly time series of observed and simulated inflow were prepared and presented in Figure 10. A good match between the monthly observed and simulated inflow is observed. Finally, the model performance is evaluated using statistical indices, as shown in Table 5. The model's error is low, and the association of observed and simulated inflow is high. Besides, the NSE value is 0.74, and the RSE is 0.51. These together indicate a good performance of the model.

4.2 Mike NAM Model Validation

The calibration of the model is validated with inflow data for the period 2012-2015 to show the capability of the model in forecasting inflow for unknown rainfall. Both numerical and graphical approaches are used to evaluate the model performance during the validation period. Graphs are prepared for the validation period similar to those prepared for the calibration period. Figure 11 shows daily observed and simulate inflow to Tenmengor reservoir during the validation period. The ability of the model to simulate peak flow is presented in Figure 12 that shows the observed and simulated inflow hydrographs from December 2012 to April 2013. The figures show that the model can simulate the daily inflow with good accuracy. The peak flow during high rainfall events can be reliability simulated by the model.

Scatter plots (Figure 13) during model validation also shows good accuracy of the simulated inflow in replicating observed inflow. The log-scale scatter plot (Figure 13b) shows that almost all the values are very close to the diagonal line of the plot. The relative residual plot (Figure 14) shows almost zero relative residuals for all the flows. The monthly time series of observed and simulated inflow (Figure 15) shows a good match for nearly the whole calibration period.

4.3. **Model Application**

4.3.1. Rainfall Intensity Duration Frequency (IDF) Curves

The IDF curves are generated in this study using the areal rainfall data of the Tenmengor catchment. Gumbel PDF is then used to estimate the maximum rainfall intensity for different durations for the return periods of 5, 10, 20, 50, 100, 500 and 1000 years. The estimated rainfall depth using the IDF curves for different return periods are given in Table 6.

4.3.2. PMP Hyetograph

PMP Hyetograph is prepared using data of 1-day rainfall as the ordinate and the duration of the rainfall as the abscissa to examine the peak rainfall time and the temporal pattern of the rainfall. Figure 16 reveals that the highest 1-hour rainfall is observed for 11 hrs, 12 hrs, and 13 hrs in a day where the rainfall exceeds 31.014 mm in 1 day, for which the PMP value is 402.445mm. These rainfall values were used as input in the calibrated and validated stages of the Mike NAM rainfall-runoff model. The obtained values are multiplied with the fraction of 1-day rainfall to obtain PMF, as shown in Figure 16.

4.4. Climate Change Impact on PMF

Rainfall projections of the study area for 2010-2099 by RegHCM-PM are used to assess the impact of climate change on inflow and PMF. The PMF is estimated for two future periods, 2031-2045 and 2061-2075, for representative concentration pathway (RCP) 8.5. RCP8.5 is used in this study to show the maximum possible impact on PMF in the study catchment due to climate change. Extreme rainfall data during those periods are used in the Mike NAM model to generate inflow. The generated data is then used for the generation of PMF data for future periods. Finally, the projected PMF data is compared with that obtained one for the observed period (2001-2015) to assess the impact of climate change on floods in the Tenmengor catchment.

Figure 17(a) shows the estimated PMF hydrograph for 1-day storm duration for the period (2001 – 2015), while Figures 17 (b) and (c) show the PMF hydrograph for the periods 2031 – 2045 and 2061 – 2075, respectively. The summary of the results obtained using PMF hydrograph for 1-day storm duration for Temengor catchment is presented in Table 7.

5. Conclusion

This study was conducted to assess the impacts of climate change on PMF in the Tenmengor catchment located in peninsular Malaysia. The study provided an understanding of PMF changes due to changes in rainfall in a tropical region where extreme rainfall is more sensitive to global warming-induced temperature rise. A large increase in PMF (48.9% and 122.6% during 2031–2045 and 2060–2075 respectively) has been projected for the Tenmengor catchment. The increase is mainly due to the large increase in PMP in the catchment. The study corresponds to the previous findings that extreme rainfall would increase more in the tropical region than in other parts of the globe, which would cause more devastating floods. Policymakers can use the finding of the study for decision making related to climate change adaptation planning. The information derived in this study can also be used to design critical hydraulic infrastructure to mitigate floods. The rainfall projections used in this study is based on the dynamical downscaling of only one GCM through a regional climate model. A large uncertainty is associated with GCM simulation, and therefore, rainfall projections of other GCMs can be used to assess changes in PMF and the associated uncertainty. The study can also be conducted to assess the changes in PMF for different emission scenarios to facilitate better decision-making on designing factors of hydraulic structures.

Declarations

Acknowledgement

The authors are grateful to the Department of Irrigation and Drainage (DID), Malaysia, for providing rainfall and streamflow data, and the National Hydraulic Research Institute (NAHRIM), Malaysia, for providing climate change simulation data.

Declaration

The authors declare that this paper is the result of our analysis and compilation. The paper is solely based on the collected data mentioned in the text. All the authors contributed to the work.

Conflict of Interest

The authors declare no conflict of interest.

Funding Statement

The author declares that no funding was received to complete this research from any organization

Author's Contribution

Conceptualization: [Saad Sh. Sameen and L. M. Sidek]; Methodology: [T. A., Mohammed and Abdul Halim Ghazali]; Formal analysis and investigation: [Shamsuddin Shahid, S. I. Abba, Anurag Malik]; Writing the first draft: [Saad Sh. Sameen and L. M. Sidek]; Editing: [Shamsuddin Shahid and Anurag Malik]

Availability of data and material

The datasets presented in the article are available from the corresponding author on reasonable request.

Code availability

The software used in this study is mentioned in the text. The software is commercially available.

Ethics approval

All authors provided ethical approval to submit the manuscript. Approval from any funding agency is not applicable since no funds were received for this study.

Consent to participate

The author has the consent to participate in the review process of this manuscript

Consent for publication

All authors provided consent to the publication of the article in TAAC.

References

Artificial Neural Networks in Hydrology. I: Preliminary Concepts. (2000). *Journal of Hydrologic Engineering*, *5*(2), 115–123. https://doi.org/10.1061/(asce)1084-0699(2000)5:2(115)

Bakhtiari, B. (2018). *Probable Maximum Precipitation Estimation in a Humid Climate*. https://doi.org/10.5194/nhess-2018-38-ac1

Beven, K. (2012). *Rainfall-Runoff Modelling*. https://doi.org/10.1002/9781119951001

Change, I. P. on C. (2014). *Climate Change 2014 Mitigation of Climate Change*. https://doi.org/10.1017/cbo9781107415416

Choi, Y. S., Shin, M.-J., & Kim, K. T. (2020). A Study on a Simple Algorithm for Parallel Computation of a Grid-Based One-Dimensional Distributed Rainfall-Runoff Model. *KSCE Journal of Civil Engineering*, *24*(2), 682–690. https://doi.org/10.1007/s12205-020-2458-z

Ciupak, M., Ozga-Zielinski, B., Adamowski, J., Deo, R. C., & Kochanek, K. (2019). Correcting Satellite Precipitation Data and Assimilating Satellite-Derived Soil Moisture Data to Generate Ensemble Hydrological Forecasts within the HBV Rainfall-Runoff Model. *Water*, *11*(10), 2138. https://doi.org/10.3390/w11102138

Ehteram, M., Binti Othman, F., Mundher Yaseen, Z., Abdulmohsin Afan, H., Falah Allawi, M., Bt. Abdul Malek, M., … El-Shafie, A. (2018). Improving the Muskingum Flood Routing Method Using a Hybrid of Particle Swarm Optimization and Bat Algorithm. *Water*, *10*(6), 807. https://doi.org/10.3390/w10060807

Farzin, S., Singh, V., Karami, H., Farahani, N., Ehteram, M., Kisi, O., … El-Shafie, A. (2018). Flood Routing in River Reaches Using a Three-Parameter Muskingum Model Coupled with an Improved Bat Algorithm. *Water*, *10*(9), 1130. https://doi.org/10.3390/w10091130

Ferraro, D., Costabile, P., Costanzo, C., Petaccia, G., & Macchione, F. (2020). A spectral analysis approach for the a priori generation of computational grids in the 2-D hydrodynamic-based runoff simulations at a basin scale. *Journal of Hydrology*, *582*, 124508. https://doi.org/10.1016/j.jhydrol.2019.124508

Gan, F., He, B., & Qin, Z. (2020). Hydrological response and soil detachment rate from dip/anti-dip slopes as a function of rock strata dip in karst valley revealed by rainfall simulations. *Journal of Hydrology*, *581*, 124416. https://doi.org/10.1016/j.jhydrol.2019.124416

Goly, A., & Teegavarapu, R. S. V. (2013). Multi-Objective Optimization Methods for Bias Correction of Statistically Downscaled Precipitation. *World Environmental and Water Resources Congress 2013*. https://doi.org/10.1061/9780784412947.116

Kimura, N., Kiri, H., Kanada, S., Kitagawa, I., Yoshinaga, I., & Aiki, H. (2019). Flood Simulations in Mid-Latitude Agricultural Land Using Regional Current and Future Extreme Weathers. *Water*, *11*(11), 2421. https://doi.org/10.3390/w11112421

Li, Z., Shi, X., Tang, Q., Zhang, Y., Gao, H., Pan, X., … Zhou, P. (2020). Partitioning the contributions of glacier melt and precipitation to the 1971–2010 runoff increases in a headwater basin of the Tarim River. *Journal of Hydrology*, *583*, 124579. https://doi.org/10.1016/j.jhydrol.2020.124579

Ling, L., Yusop, Z., Yap, W.-S., Tan, W. L., Chow, M. F., & Ling, J. L. (2019). A Calibrated, Watershed-Specific SCS-CN Method: Application to Wangjiaqiao Watershed in the Three Gorges Area, China. *Water*, *12*(1), 60. https://doi.org/10.3390/w12010060

Mohamadi, S., Sammen S. S., Panahi, F. et al. Zoning map for drought prediction using integrated machine learning models with a nomadic people optimization algorithm. Nat Hazards 104, 537–579 (2020). https://doi.org/10.1007/s11069-020-04180-9

Noji, E. K. (1991). Natural Disasters. *Critical Care Clinics*, *7*(2), 271–292. https://doi.org/10.1016/s0749-0704(18)30306-3

Ohl, C. A., & Tapsell, S. (2000). Flooding and human health. *BMJ (Clinical Research Ed.)*, *321*(7270), 1167–1168. https://doi.org/10.1136/bmj.321.7270.1167

Ren, X., Hong, N., Li, L., Kang, J., & Li, J. (2020). Effect of infiltration rate changes in urban soils on stormwater runoff process. *Geoderma*, *363*, 114158. https://doi.org/10.1016/j.geoderma.2019.114158

Rientjes, T. H. M., Muthuwatta, L. P., Bos, M. G., Booij, M. J., & Bhatti, H. A. (2013). Multi-variable calibration of a semi-distributed hydrological model using streamflow data and satellite-based evapotranspiration. *Journal of Hydrology*, *505*, 276–290. https://doi.org/10.1016/j.jhydrol.2013.10.006

Pham, Q.B., Mohammadpour, R., Linh, N.T.T. et al. Application of soft computing to predict water quality in wetland. Environ Sci Pollut Res 28, 185–200 (2021). https://doi.org/10.1007/s11356-020-10344-8

Sammen S. S.; Ghorbani, M.A.; Malik, A.; Tikhamarine, Y.; AmirRahmani, M.; Al-Ansari, N.; Chau, K.-W. Enhanced Artificial Neural Network with Harris Hawks Optimization for Predicting Scour Depth Downstream of Ski-Jump Spillway. *Appl. Sci.* 2020, *10*, 5160. https://doi.org/10.3390/app10155160

Smith, H. F. (1965). Handbook of Applied Hydrology. A compendium of water-resources technology. Van Te Chow, Ed. McGraw-Hill, New York, 1964. 1418 pp. Illus. $39.50. *Science*, *148*(3667), 219. https://doi.org/10.1126/science.148.3667.219

Song, J.-H., Her, Y., Suh, K., Kang, M.-S., & Kim, H. (2019). Regionalization of a Rainfall-Runoff Model: Limitations and Potentials. *Water*, *11*(11), 2257. https://doi.org/10.3390/w11112257

Tikhamarine, Y., Malik, A., Pandey, K. et al. Monthly evapotranspiration estimation using optimal climatic parameters: efficacy of hybrid support vector regression integrated with whale optimization algorithm. Environ Monit Assess 192, 696 (2020). https://doi.org/10.1007/s10661-020-08659-7

Torabi Haghighi, A., Sadegh, M., Behrooz-Koohenjani, S., Hekmatzadeh, A. A., Karimi, A., & Kløve, B. (2019). The mirage water concept and an index-based approach to quantify causes of hydrological changes in semi-arid regions. *Hydrological Sciences Journal*, *65*(2), 311–324. https://doi.org/10.1080/02626667.2019.1691728

Velázquez-Zapata, J. A. (2019). Comparing Meteorological Data Sets in the Evaluation of Climate Change Impact on Hydrological Indicators: A Case Study on a Mexican Basin. *Water*, *11*(10), 2110. https://doi.org/10.3390/w11102110

Vitousek, S., Barnard, P. L., Fletcher, C. H., Frazer, N., Erikson, L., & Storlazzi, C. D. (2017). Doubling of coastal flooding frequency within decades due to sea-level rise. *Scientific Reports*, *7*(1), 1399. https://doi.org/10.1038/s41598-017-01362-7

Yang, X., Magnusson, J., Huang, S., Beldring, S., & Xu, C.-Y. (2020). Dependence of regionalization methods on the complexity of hydrological models in multiple climatic regions. *Journal of Hydrology*, *582*, 124357. https://doi.org/10.1016/j.jhydrol.2019.124357

Tables

Please see the supplementary files section to view the tables.

Figures

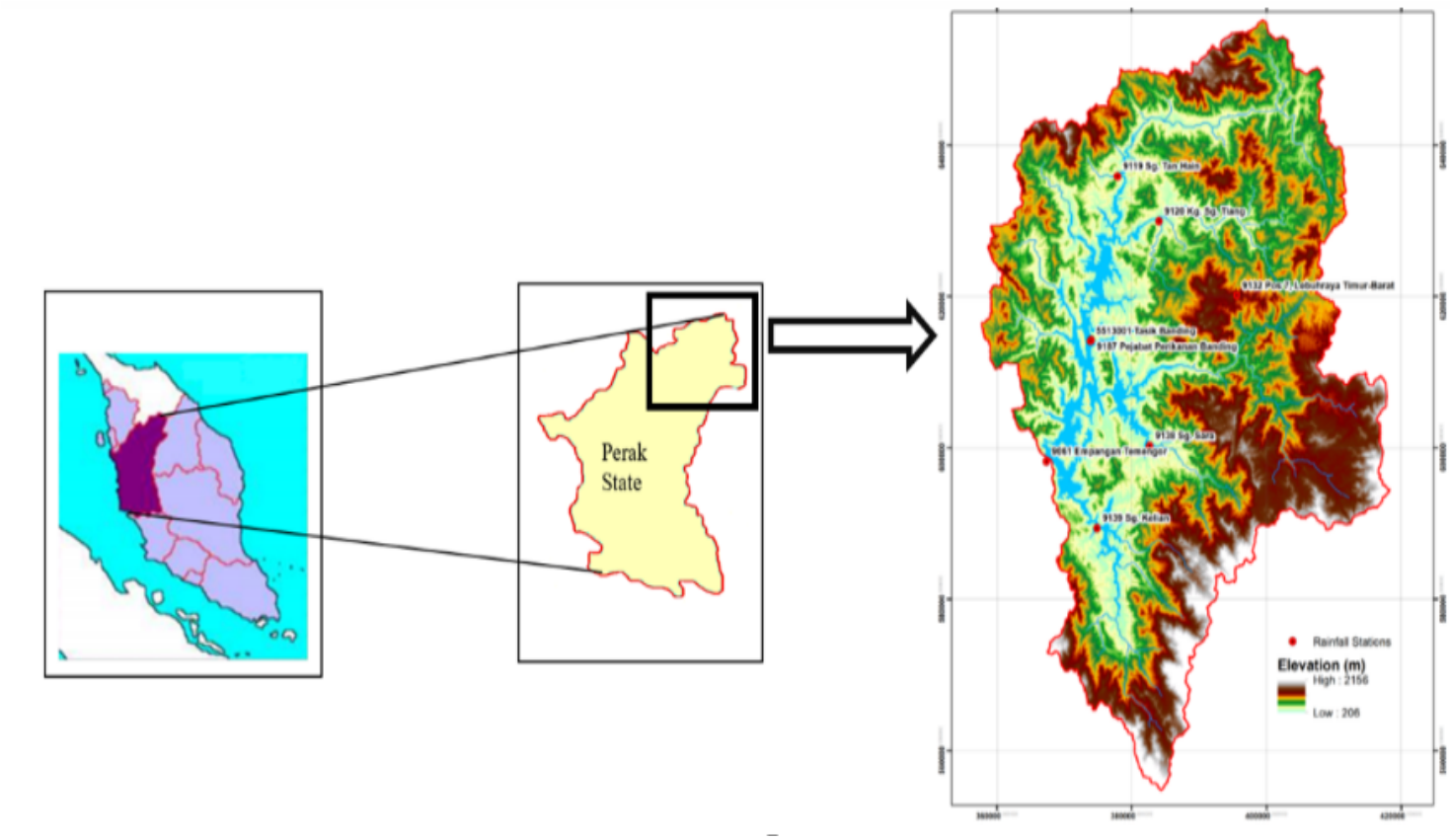

Figure 1

Location of Temengor catchment in Peninsular Malaysia.

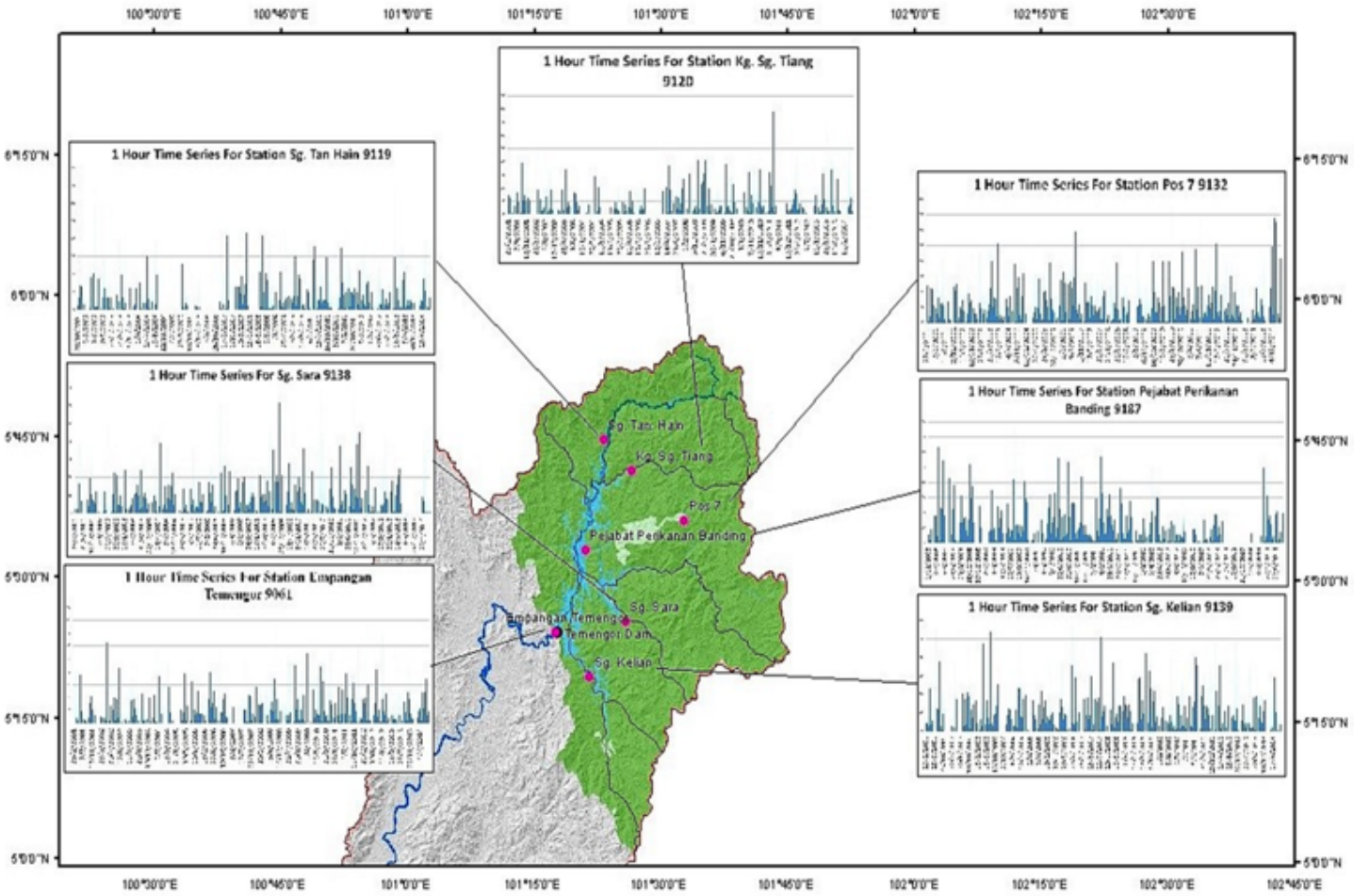

Figure 2

Time series of rainfall data at different locations of the Temenggor dam catchment area

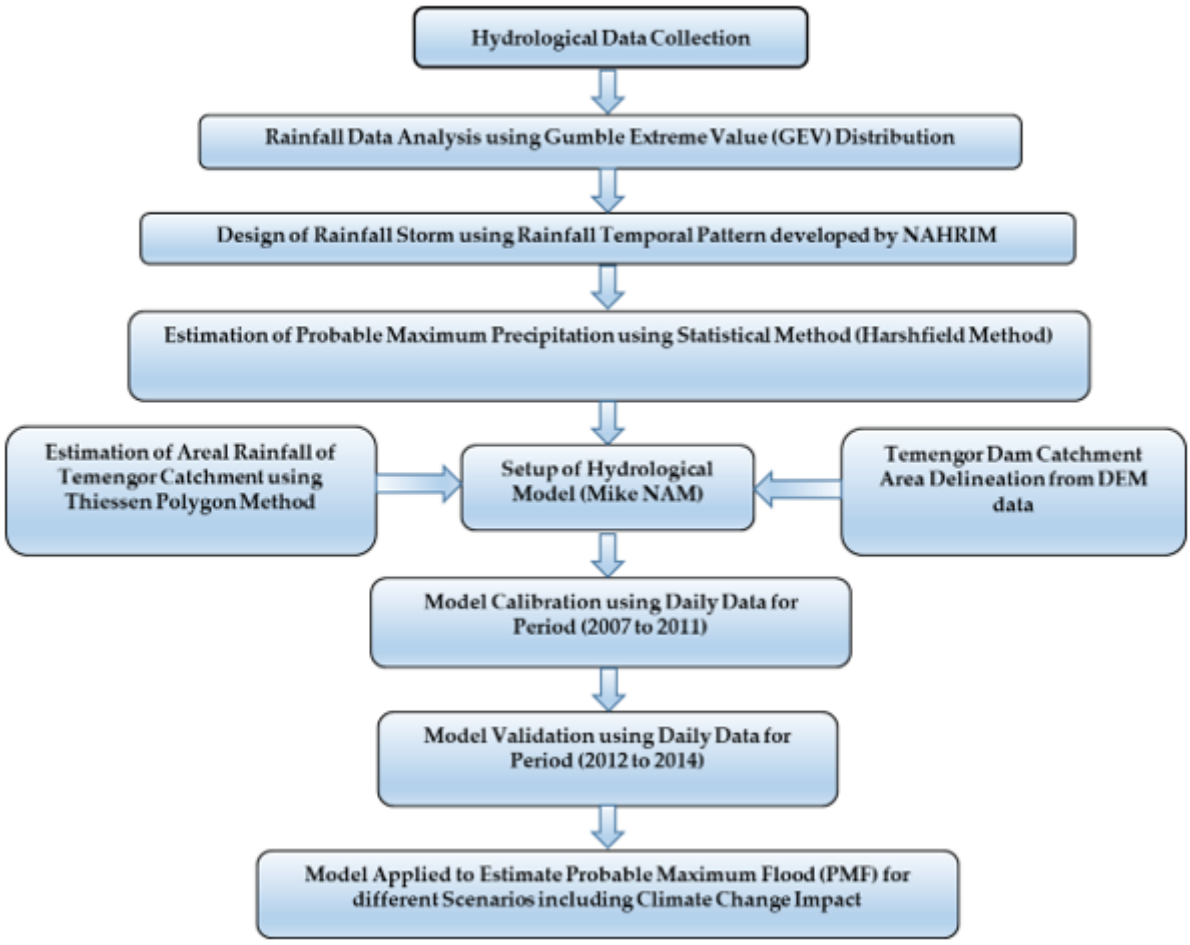

Figure 3

Methodology used for hydrological modeling of Temengor catchment.

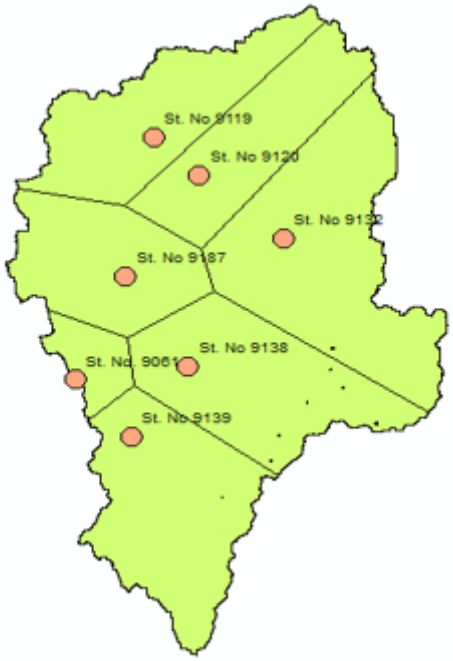

Figure 4

Thiessen polygons derived based on rainfall gauges in the study area.

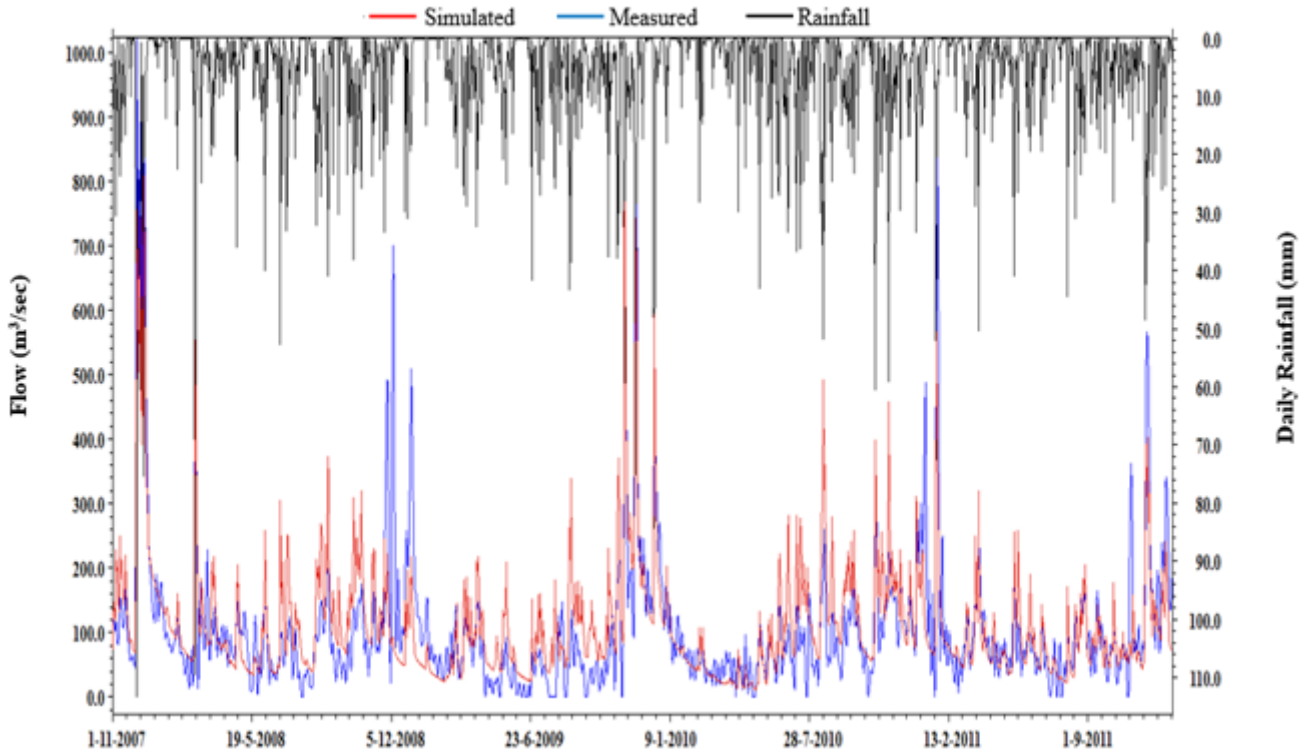

Figure 5

Observed and simulated daily inflow to Temenggor reservoir during model calibration (2007-2011).

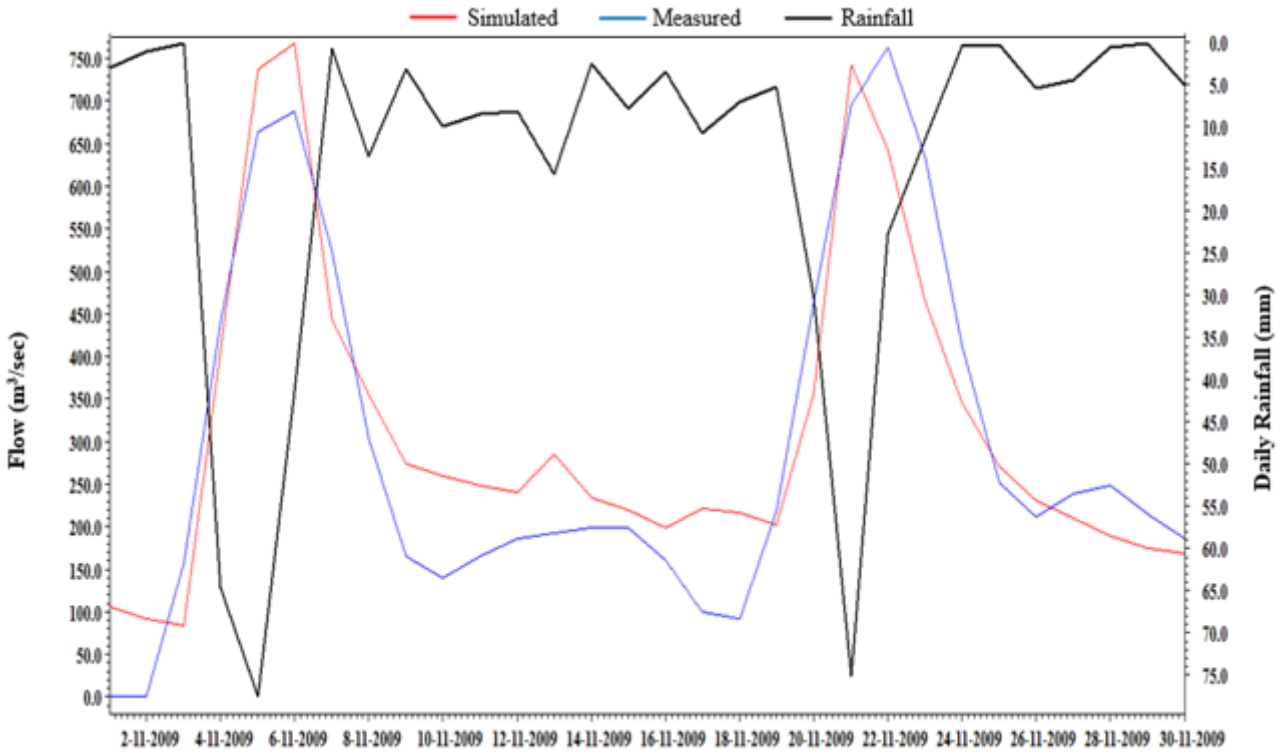

Figure 6

Observed and simulated peak flow by the calibrated Mike NAM model in Temengor catchment in November 2009.

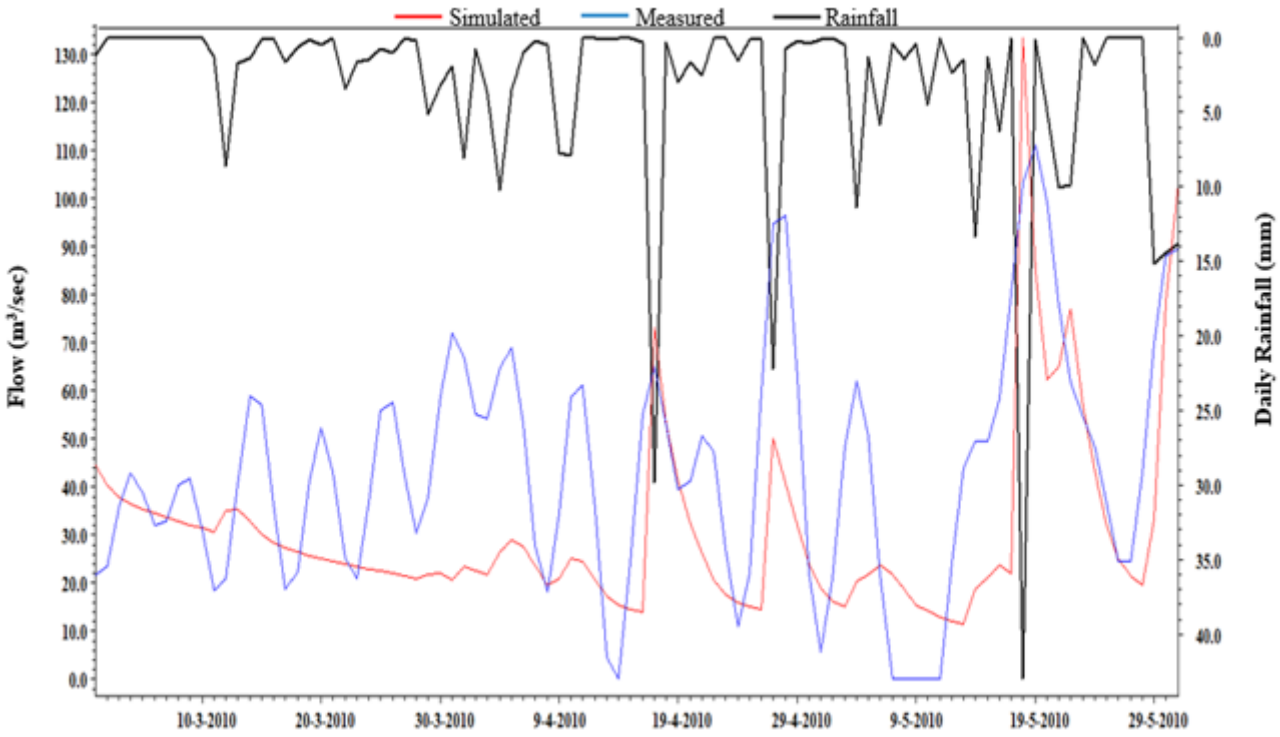

Figure 7

Observed and simulated low flow estimated by the calibrated Mike NAM model in Temengor catchment during March to June 2010.

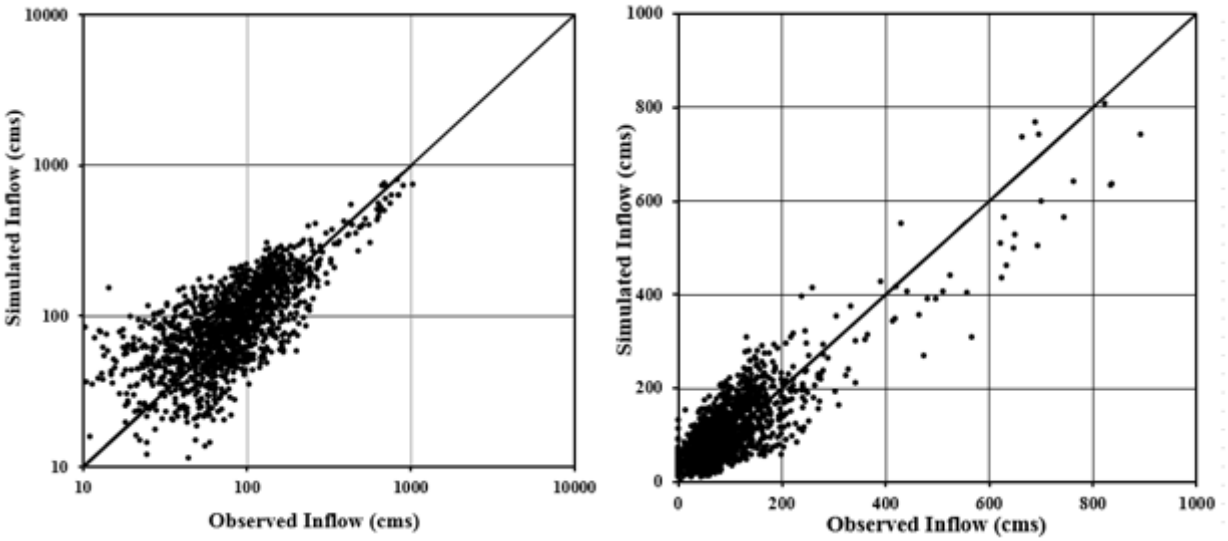

Figure 8

Scatter plot of daily observed and simulated inflow during the calibration period, (a) Normal scale; (b) Logarithmic scale

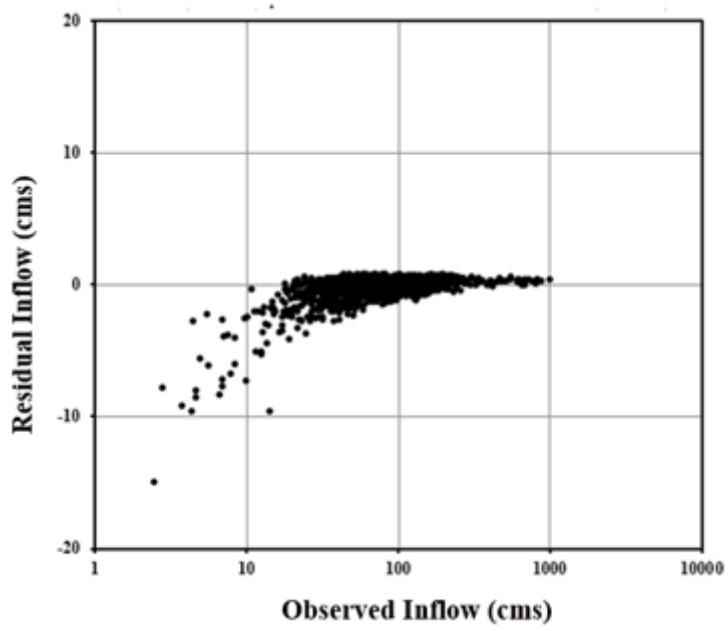

Figure 9

Relative residual plot of daily inflow during model calibration

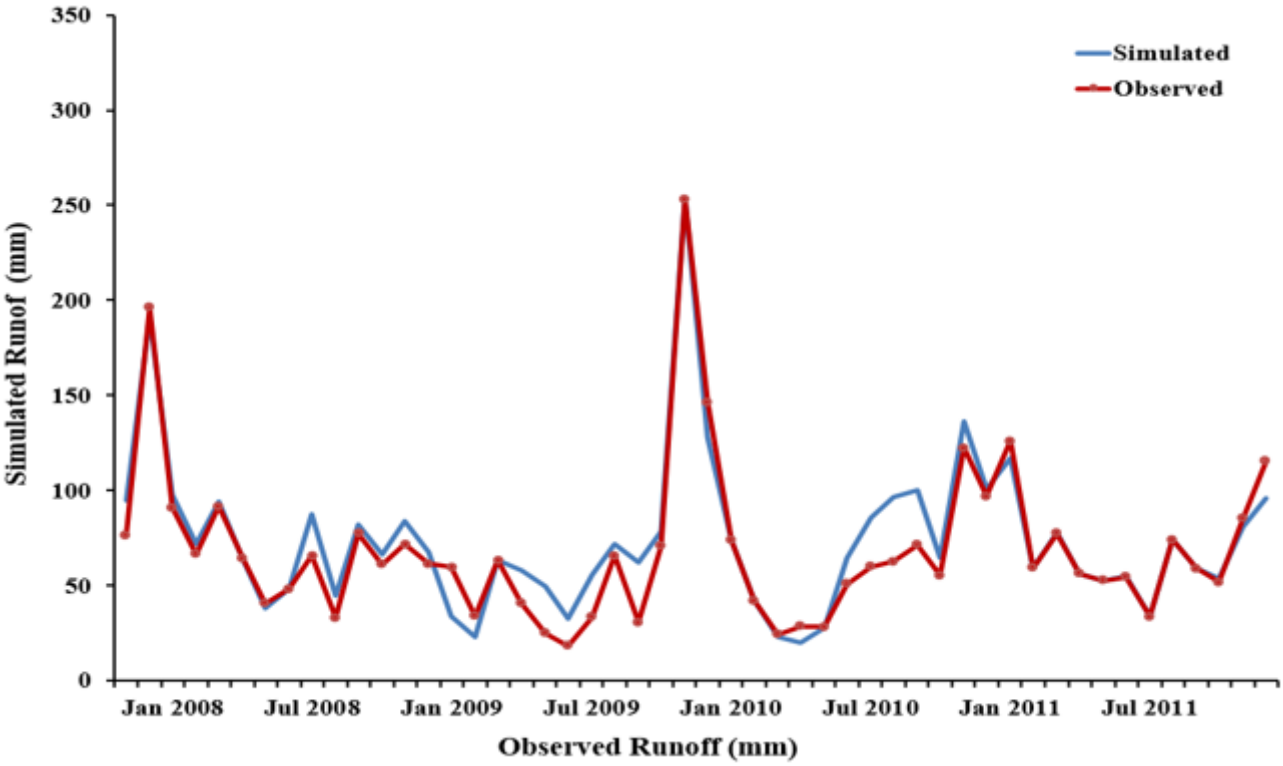

Figure 10

Monthly observed and simulated inflow to Tenmengor reservoir during model calibration

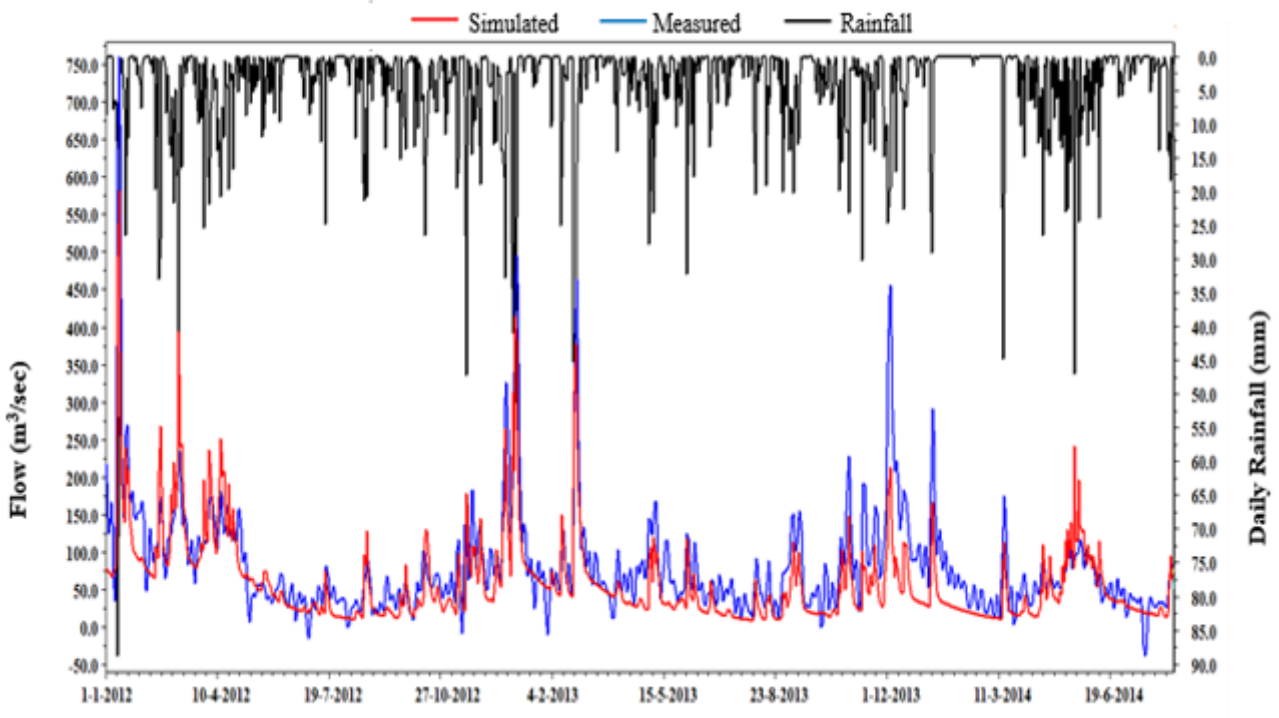

Figure 11

Observed and simulated daily inflow during model validation (2012-2014).

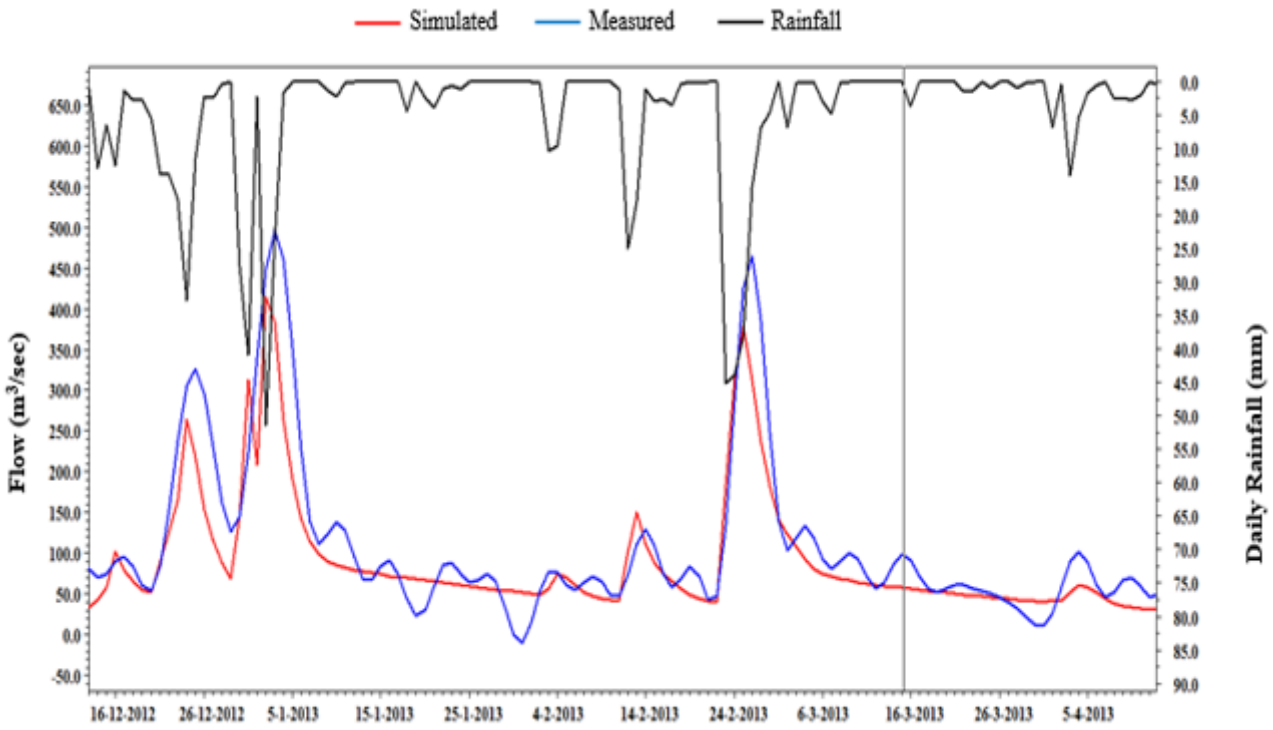

Figure 12

Observed and simulated peak flow during Dec. 2012 to Apr. 2013.

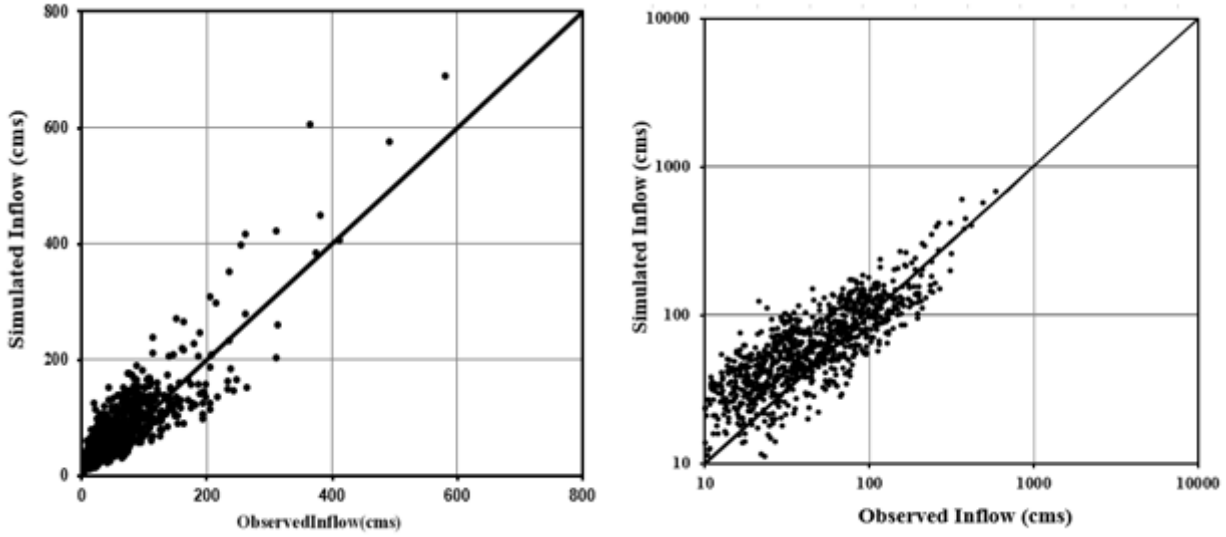

Figure 13

Scatter plot of daily observed and simulated inflow during the validation period, (a) normal scale; (b) logarithmic scale

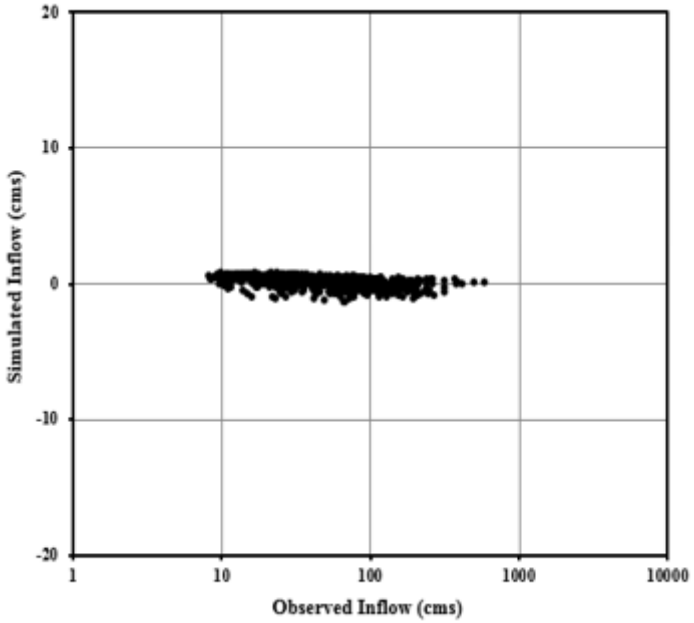

Figure 14

Relative residual plot of daily inflow during model validation

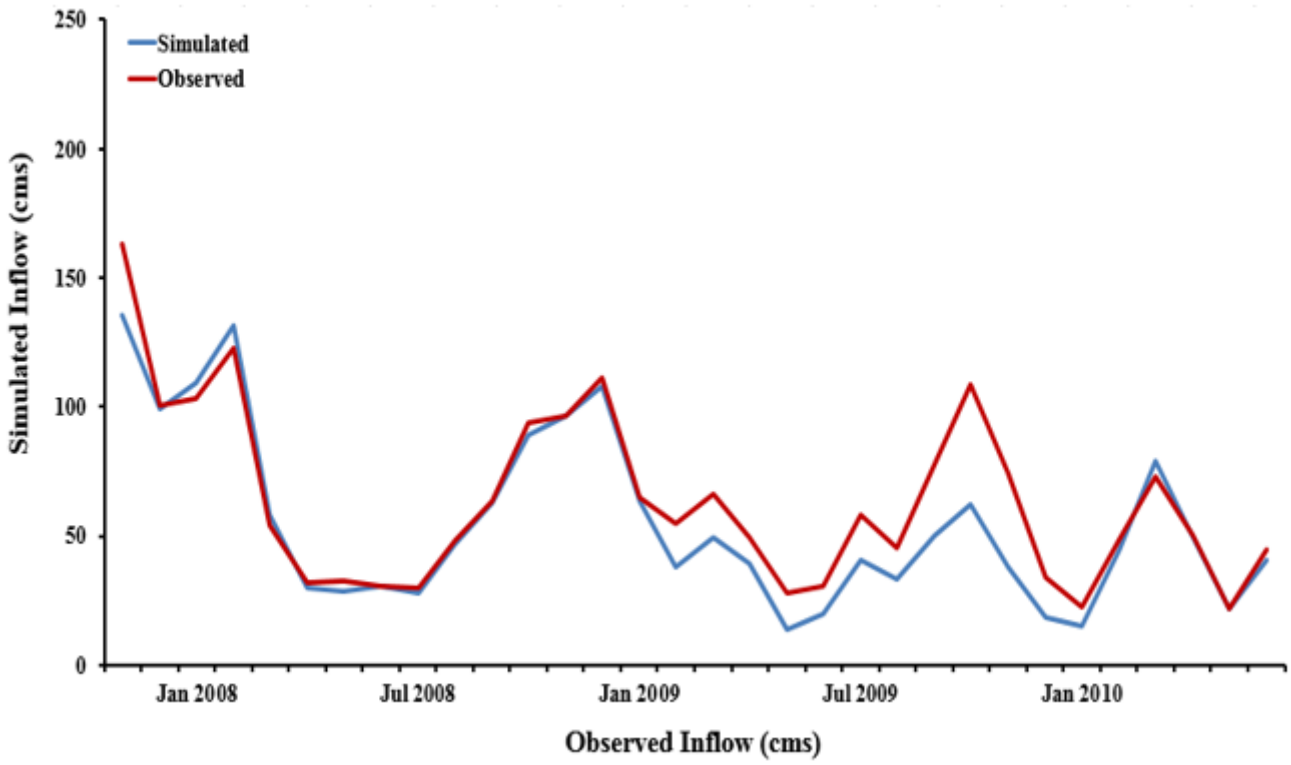

Figure 15

Monthly observed and simulated inflow during model calibration

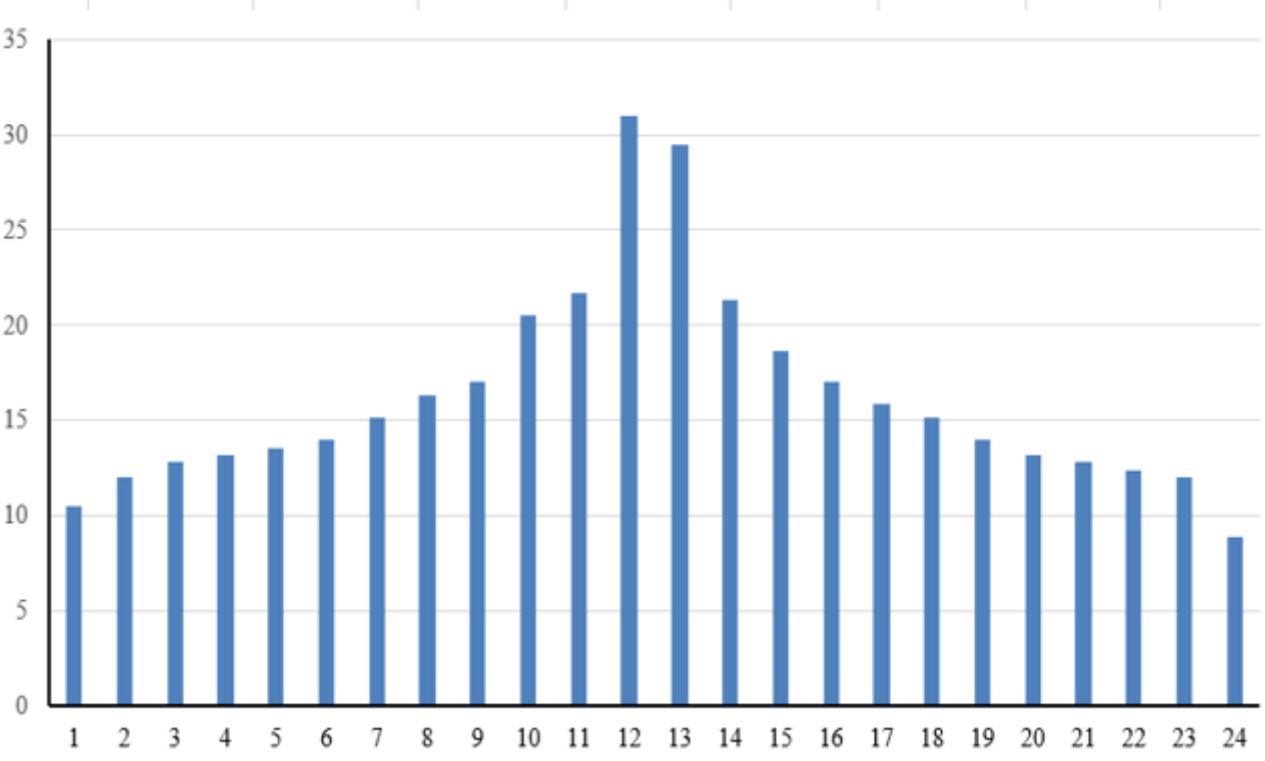

Figure 16

Temporal pattern of Probable Maximum Precipitation in Temenggor catchment

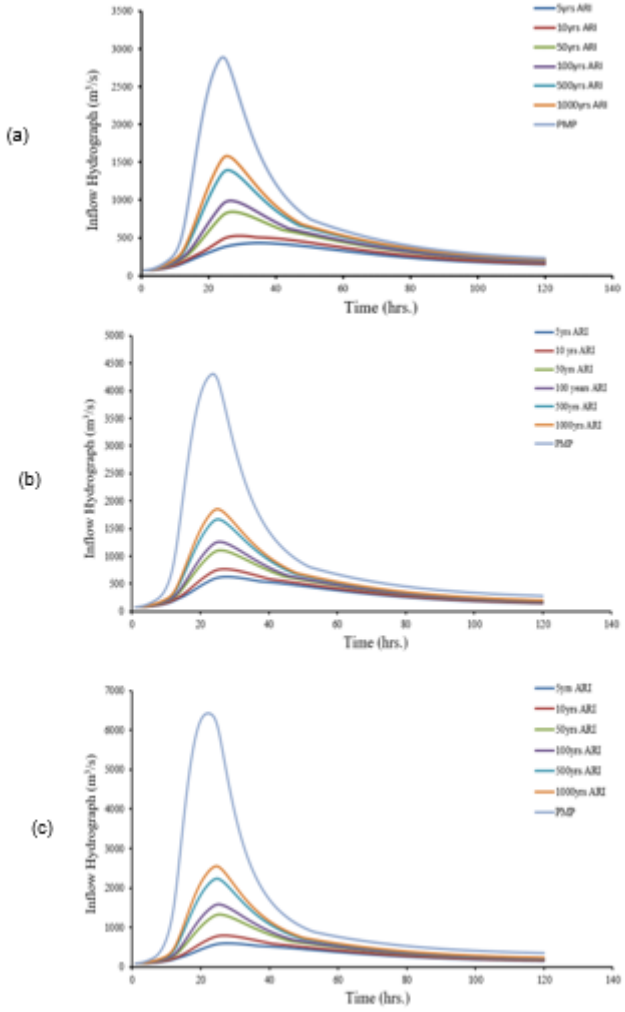

Figure 17

Probable maximum flood hydrograph for the Temenggor catchment for the period (a) 2001 – 2015; (b) 2031 – 2045; and (c) 2061 – 2075

Supplementary Files

This is a list of supplementary files associated with this preprint. Click to download.

- Table.docx